

# Finite Element modeling of Nomex<sup>®</sup> honeycomb cores : Failure and effective elastic properties

L. Gornet, S. Marguet, and G. Marckmann

**Abstract** The purpose of the present study is to determine the components of the effective elasticity tensor and the failure properties of Nomex<sup>®</sup> honeycomb cores. In order to carry out this study, the NidaCore software, a program dedicated to Nomex<sup>®</sup> Cores predictions, has been developed using the Finite Element tool Cast3M-CEA. This software is based on periodic homogenization techniques and on the modelling of structural instability phenomena. The homogenization of the periodic microstructure is realized thanks to a strain energy approach. It assumes the mechanical equivalence between the microstructures of a RVE and a similar homogeneous macroscopic volume. The key point of the modelling is that by determining the RVE buckling modes, the ultimate stress values of the homogenized core can be deduced. The numerical analysis shows an adequation between the first critical buckling modes computed and the ultimate stress values experimentally observed in standardized tests. This approach, strengthened by experimental data, makes it possible to devise a failure criterion. This criterion relies on the understanding of the mechanical effects caused by a local damage. In order to improve the reliability of the software, predicted mechanical properties are compared with data given by the Euro-Composite company and with results coming from crushing tests performed on sandwich specimens. This study brings out a powerful tool for the determination of the mechanical properties of most Nomex<sup>®</sup> honeycomb core used in nautical construction. The design of oceanic sailing race boats is one of its most outstanding practical applications.

**keyword:** Manuscript, preparation, typeset, format, CMES.

## 1 Introduction

The structural composite sandwich panels are extensively used in lightweight constructions. A typical structural sandwich panel consists of a honeycomb core covered on both sides by laminate face-sheets. The aim of the present study is to propose and develop the numerical determination of the effective stress-strain behaviour of Nomex<sup>®</sup> honeycomb cores. These honeycombs are extensively used in the manufacturing of aerospace structures and of oceanic sailing race boats. Sandwich structures under consideration are made of carbon-fiber epoxy-matrix composite laminate face-sheets and Nomex<sup>®</sup> cores. The understanding of the

behaviour and eventually of the failure of honeycomb cores is extremely important for the design of these engineering composite sandwich structures. The predictions of the mechanical honeycomb core properties are directly related to the structural integrity and safety requirements of the entire lightweight structure

Since the pioneering work on determination of the effective mechanical properties for two-dimensional cores [Kelsey, Gellatley and Clark (1958), Gibson and Ashby (1988)], numerous studies of cellular sandwich cores have been recently published [Hohe, and Becker (1999) and (2001), Grediac (1991), ]. In this context the NidaCore software dedicated to Nomex<sup>®</sup> cores was developed in order to predict the failure conditions of these honeycomb cores [Gornet, Marckmann and Lombard (2006)]. The NidaCore software has been developed to determine the three dimensional mechanical properties of the core. The elastic mechanical properties are determined by a three-dimensional Finite Element model that involves periodic homogenization techniques. For the homogenization of the honeycomb microstructure, a strain energy-based concept is used. It assumes the macroscopic mechanical equivalence of a Representative Volume Element for the given microstructure with a similar homogeneous volume element. The software has been developed using the Finite Element tool Cast3M-CEA. In the present study, numerical Nomex<sup>®</sup> cores predictions are compared with the experimental data given by the Euro-Composites company.

The original key point of the modelling is that by determining the RVE buckling modes, the ultimate stress values of the homogenized core can be deduced. Based on buckling modes, numerical instability analysis reproduces the ultimate stresses experimentally observed on standard test methods. This approach, strengthened by experimental data, makes it possible to devise a failure criterion. This criterion relies on the understanding of the mechanical effects caused by a local damage. In order to go further, the skin effect influence on Nomex<sup>®</sup> properties is discussed for T700/M10 face-sheets made of carbon-fibre epoxy-matrix cross-ply or angle-ply laminates (Fig. 1)



**Figure 1:** Sandwich, hexagonal Nomex<sup>®</sup> core and carbon-fibre epoxy-matrix face-sheets

## 1 Strain energy based concept for homogenization

Periodic homogenization consists in substituting to a strongly heterogeneous medium, a fictitious homogeneous one which is expected to be equivalent in the largest range of loadings. Based on this assumption, our Finite Element software NidaCore has been developed to determine the three dimensional mechanical Nomex<sup>®</sup> cores properties. Hexagonal and rectangular over-expanded honeycomb cores are investigated. Over-expanded cores are intensively used for shell geometries due to their deformability abilities.

### 1.1 Representative Volume Element

The Representative Volume Elements adopted for the homogenization of the hexagonal and rectangular over-expanded honeycomb cores are presented on Fig. 2. Any larger volume can be obtained by successive translations of the RVE. In the case of the RVE represented on figure 2, (1,2,3) axis corresponds to the orthotropic basis of the homogeneous volume element.

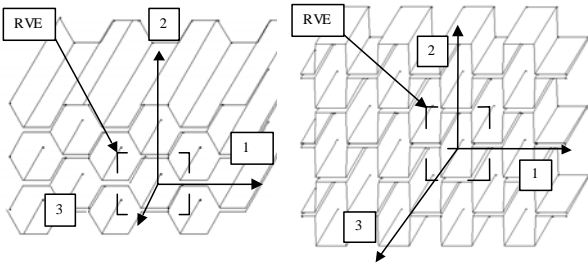


**Figure 2 :** Hexagonal and over-expanded honeycomb cores

### 1.2 Periodic homogenization

The mathematical process which allows to pass from the global variables defined on the RVE to the local ones is called the localization process. By considering  $Y$  the RVE and  $|Y|$  its volume measurement, the space average of a

second order tensor  $X_{ij}$  (strain or stress) is given by the equation (Eq. 1).

$$\langle X_{ij} \rangle = \frac{1}{|Y|} \int_Y X_{ij}(y) dy \quad (1)$$

The average stress and strain tensors are noted respectively  $\Sigma_{ij} = \langle \sigma_{ij} \rangle$  and  $E_{ij} = \langle \varepsilon_{ij} \rangle$ . Periodic homogenization is based on the data of the average strain field and results in determining the compliance operator  $C^{RVE}$  of the RVE imposing displacement boundary conditions on its edge  $\partial Y = \partial Y_{21} \cup \partial Y_{22}$ . Where  $\partial Y_{21}$  represents free-edges and  $\partial Y_{22}$  displacement boundary condition surfaces. The homogenization process proposed hereafter is based on the resolution of six elementary linear elasticity problems (2). It must be highlighted that for periodic homogenization, stress or strain approaches are equivalent [Suquet (1982)]. The NidaCore software is based on a strain driven periodic homogenization approach conducting to displacement boundary conditions. This method leads to six linear elasticity problems which have to be solved under strain boundary conditions, such as  $E_{kh} = 1$  and  $E_{ij} = 0$  if  $(i, j) \neq (k, h)$ . The six elementary problems to be solved on the RVE  $Y$  are derived hereafter :

$$\begin{aligned} \operatorname{div}(\sigma(y)) &= 0 & \text{in } Y \\ \sigma(y) &= C(y)\varepsilon(u(y)) & \text{in } Y \\ \varepsilon(u) &= \operatorname{grad}_s(u(y)) \\ \sigma(y)\vec{n}_{ext} &= \vec{0} & \text{on } \partial Y_{21} \\ \vec{u}(y) &= E\vec{y} + \vec{v}_{per} & \text{on } \partial Y_{22} \end{aligned} \quad (2)$$

The finite element RVE meshes are presented in Fig. 3.

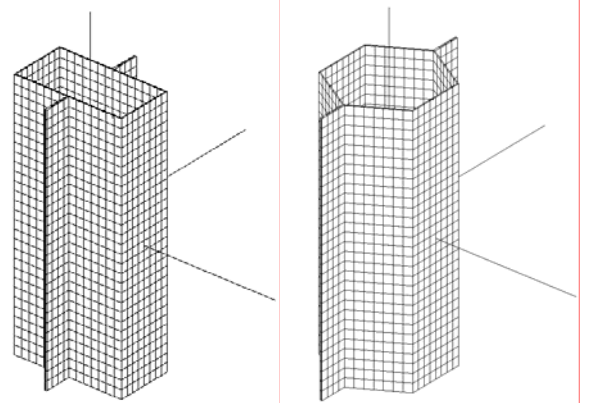


**Figure 3 :** Hexagonal and Over-expanded honeycomb RVE with orthotropic axis

The displacement field  $\vec{v}_{per}$  is periodic and of equal values on the opposite faces of the RVE. Practically, Hill-Mandel energy approach is used to calculate the equivalent homogenized stiffness components described by a six by six matrix  $C_{IJ}^{RVE}$ . The homogenised core behaviour is presented by Eq. 3

$$\begin{aligned}\Sigma &= C^{RVE} E \\ E &= S^{RVE} \Sigma\end{aligned}\quad (3)$$

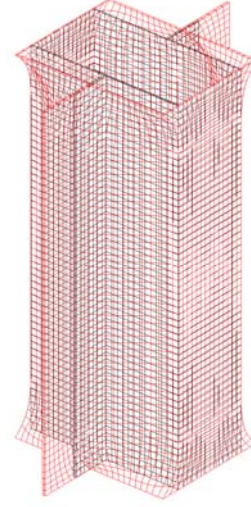
The homogenized mechanical stiffness characteristics  $C^{RVE}$  of the RVE can be simply derived with the Hill-Mandel theorem. This theorem implies that the RVE energy is equal to the average of the energies of its components (Eq. 4) :

$$\frac{1}{|Y|} \int_Y \sigma : \varepsilon dy = E : (C^{RVE} E) \quad (4)$$

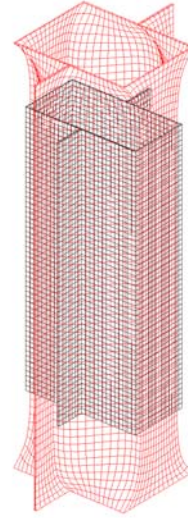
The anisotropic homogenized elastic stiffness tensor is determined by deriving the twenty one linear combinations of the six elementary problems defined on the RVE. The engineering constants, the Young's moduli, the Poisson's ratios and the shear moduli, are deduced from the RVE compliance coefficients. The present study confirms that for the honeycombs under consideration, the Representative Volume Element symmetries lead to orthotropic homogenized mechanical properties.

### 1.3 Finite Element simulations

The homogenized mechanical properties of honeycomb cores are determined from the RVE's meshes presented in figure 3. According to manufacturers information derived from their mechanical tests, the RVE retained for experimental data comparisons are 12.7mm height. Each RVE finite element model involves 41556 nodes, which represent 6156 hexahedron elements from the Serendip's family with 20 isoparametric nodes and quadratic interpolation functions. For this finite element, numerical integration is performed using 27 Gauss' points. RVE meshes include only one element in the elementary wall thickness and two in double thickness parts (Fig. 3). Convergence studies were carried out for various discretizations and the selected meshes were optimal with respect to CPU time and finite element convergence. The finite element simulations leading to the homogenized mechanical properties are carried out under the assumption of small displacements and strains. For orthotropic core under consideration, nine combinations of the six elementary problems (2) are necessary to determine the mechanical properties. Deformed shapes under the nine combinations corresponding to loadings in orthotropic axis are presented on Fig. 4 to 7.



Deformed Shape at Test Strain EPBB



Deformed Shape at Test Strai

**Figure 4:** RVE ECA-R deformed shapes for loadings  $E_{22}$ ,  $E_{22}$  and  $E_{33}$

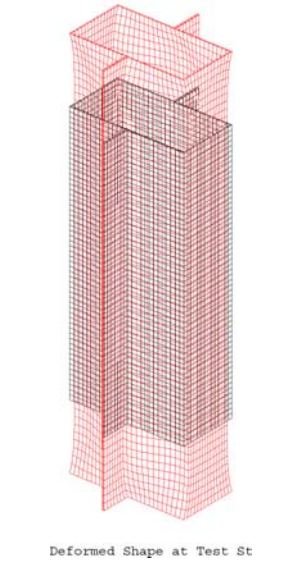
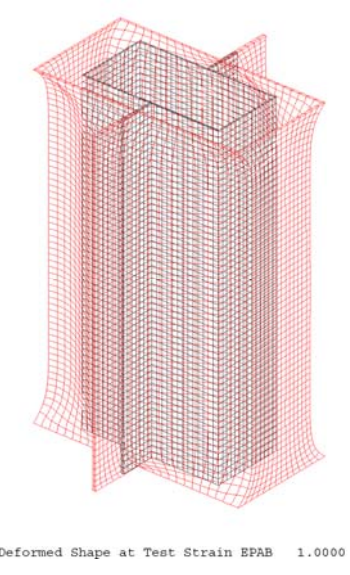
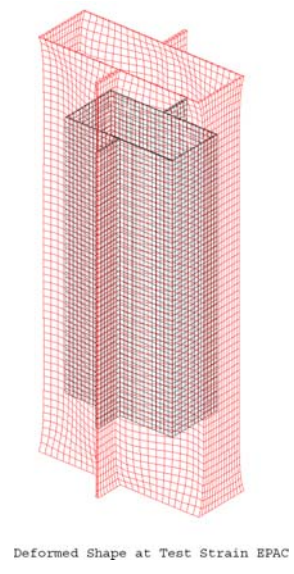
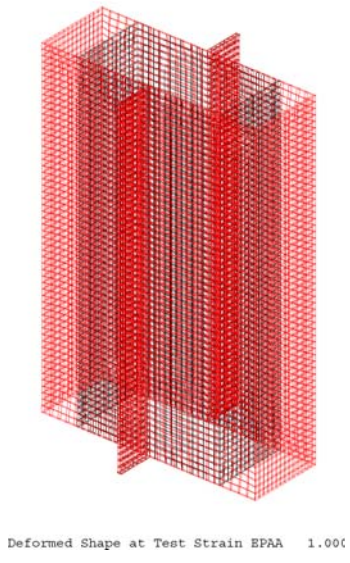


**Figure 5 :** RVE ECA-R deformed shapes under loading conditions  $E_{11}$ , and ( $E_{11}$  and  $E_{22}$ )

**Figure 6 :** RVE ECA-R deformed shapes under loading conditions ( $E_{11}$  and  $E_{33}$ ), and  $E_{33}$

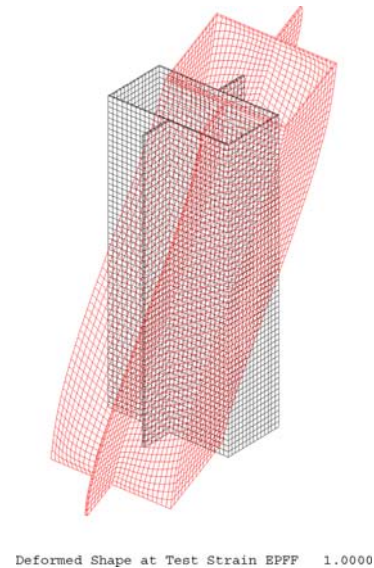
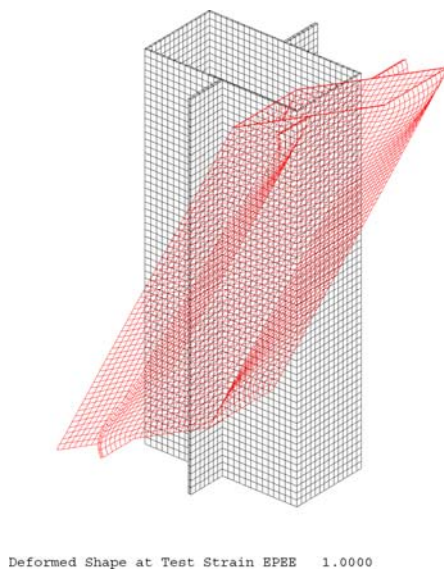


**Figure 7** : RVE ECA-R deformed shapes under loading conditions ( $E_{12}, E_{13}, E_{23}$ )

## 2 Mechanical characteristics



From the designer point of view, the honeycomb cores made of Nomex<sup>®</sup> paper are available for various densities. In this study, the mechanical characteristics of Nomex<sup>®</sup> paper are obtained by finite element model updated according to out of plan shear moduli of the homogenized core available in the Euro-Composite catalogue [Nomex<sup>®</sup> cores]. It should be highlighted that a Nomex<sup>®</sup> core may have different densities for the same geometric dimensions because of the variation of the resin amount deposited during the industrial process. This method leads to create more resistant cores. The manufacturers' catalogues only give the most significant mechanical properties. Core properties are generally established thanks to mechanical tests carried out with 12.7mm thickness specimens. The out of plan shear moduli  $G_{13}$  and  $G_{23}$  and associated rupture shear stresses  $\sigma_{13}^C$  and  $\sigma_{23}^C$  are the only data provided by the manufacturer with the crushing stress  $\sigma_{33}^C$ . Obviously these few experimental data are insufficient to perform three dimensional finite element analysis. Moreover, as mentioned by Hexcel documents [Hexcel (1999)], "Users should make their own assessment of the suitability of any product for the purposes required". The homogenization of periodic media above described then appears as the numerical solution to determine the three dimensional mechanical characteristics of the honeycomb cores.

## 2.1 Elastic properties

In the case of the hexagonal or rectangular over-expanded honeycombs cores, RVE symmetries lead to an orthotropic homogenized mechanical elastic behaviour. For Euro-Composite catalogue, the denomination ECA-R 4.8-29 (51) stands for a rectangular section core inscribed within a 4.8mm diameter circle with a 29 Kg/m<sup>3</sup> material density and a wall thickness of 51µm. ECA 4.8-29 (51) denomination is equivalent for an hexagonal core geometry. ECA-R 4.8-29 (51) mechanical properties established by the NidaCore software are presented in table 1. The evolutions of mechanical properties according to the core density for both hexagonal and over-expanded honeycombs are plotted in figure 8. The three dimensional core properties are included in three dimensional finite element studies dedicated to the sandwich structure shear reinforcements of oceanic sailing race boats. An example of Scarf reinforcements used on sailing race boats [6] is presented on Fig. 9.

**Table 1 :** Minimum (Min) and typical (Typ) homogenized mechanical properties of honeycomb cores ECA-R 4.8 with densities of 29, 48 and 64Kg/m<sup>3</sup> and a thickness of wall of 51µm

ECA-R	Min		Typ		Min		Typ	
	MPa	4.8-29 (51)	MPa	4.8-29 (51)	MPa	4.8-48 (51)	MPa	4.8-64 (51)
$\nu_{12}$		0.2606		0.2606		0.2606		0.2606
$\nu_{13}$		0.2240		0.2240		0.2240		0.2240
$\nu_{23}$		0.0219		0.0219		0.0219		0.0219
$E_1$	44.5	72.5	101.1	128.7	129.6	152.0		
$E_2$	4.4	7.1	9.9	12.6	12.7	14.9		
$E_3$	79.4	129.5	180.5	229.8	231.4	271.5		
$G_{12}$	0.5	0.9	1.2	1.6	1.6	1.9		
$G_{13W}$	14.6	23.9	33.3	42.4	42.7	50.1		
$G_{23L}$	8.6	14.1	19.6	25.0	25.1	29.5		

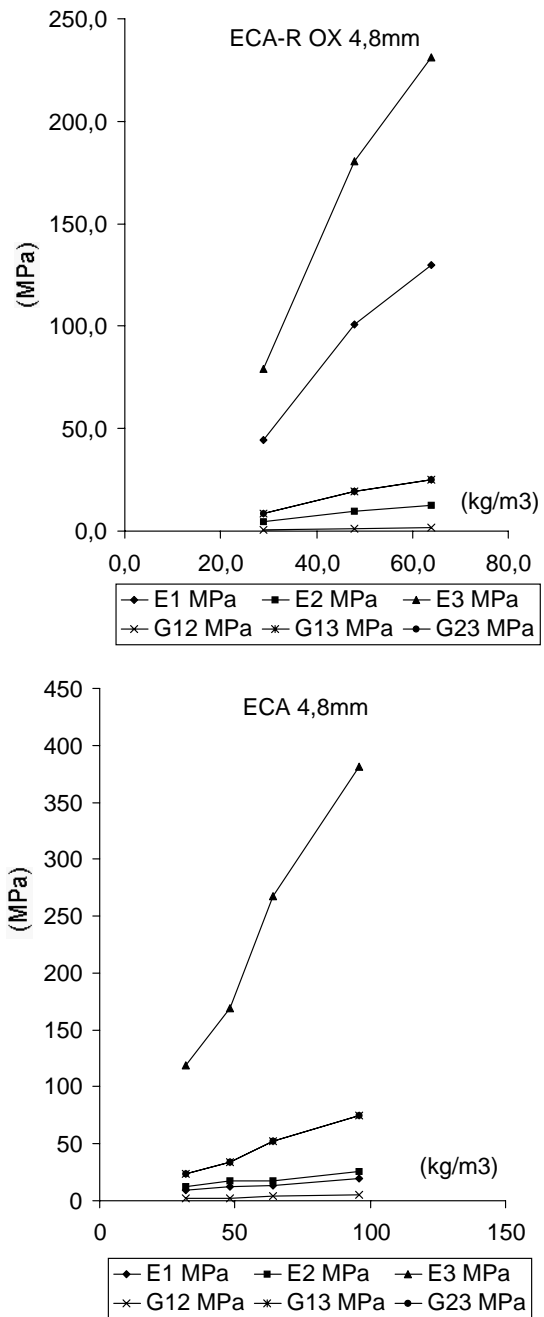


**Figure 8:** Hexagonal (ECA 4.8) and over-expanded (ECA-R 4.8) honeycomb core mechanical property evolutions with core density

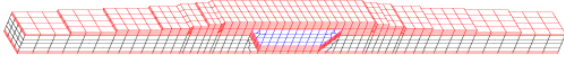


**Figure 9 :** Tridimensional Finite Element modelling of a sandwich Scarf

## 2.2 Failure stresses

Failure is often an ill-defined term in reference of Nomex<sup>®</sup> honeycomb cores. The periodic structures typically exhibit many local failures after having been exposed to structural instability. Experimentally it can be observed that the buckling corresponds to a very significant increase in the damage of the walls of the core. During mechanical shear tests or out of plan compression tests, a brutal decrease of the load appears after structural instability. This collapse corresponds to the walls crushing. Nomex<sup>®</sup> are known to have a fragile linear elastic mechanical behaviour until their critical load. In this study, it will be considered that this load corresponds to their ultimate limit. The critical strains are given for the whole cases of loadings. The study of the linear elastic buckling of the RVE leads to the identification of the failure stress properties. Buckling modes of the over-expanded honeycomb RVE under shear loadings are presented on figure 10. Core displacements are considered to be so small that the RVE geometry could be frozen to the initial unloading configuration and the stress/strain relationship could be considered to be linear. According to this assumption, Euler critical condition then reduces to a standard eigenvalue problem (Eq. 5)

$$[K + \lambda^2 K_s] \vec{X}_\lambda = \vec{0} \quad (5)$$

Where  $K$  refers to the initial unstressed configuration and coincides with the stiffness of the RVE,  $K_s$  represents the geometrical stiffness that accounts for the presence of loadings evolving linearly with  $\lambda^2$ .  $\vec{X}_\lambda$  is the eigenmode of buckling associated with the eigenvalue  $\lambda^2$ . The critical strain boundary conditions are determined by the relation (Eq. 6) and Hooke's law (Eq. 3) in order to create a pure stress loading.

$$E^c = \lambda^2 E \quad (6)$$

Failure stresses components associated with the critical strains (Eq. 6) are defined by the equation (Eq. 7)

$$\hat{\sigma}_I^c = \hat{C}_{IJ} \hat{E}_J^c \quad (7)$$

The method is derived hereafter for each stress component of an orthotropic material core. For the  $\sigma_{11}$  case, macroscopic strain loadings  $E$  are defined by components (Eq. 8).

$$\begin{aligned} E_{11} &= S_{11} \sigma_{11} \\ E_{22} &= S_{12} \sigma_{11} \\ E_{33} &= S_{13} \sigma_{11} \end{aligned} \quad (8)$$

Buckling strains are given by the equation (6) for each component and ultimate stress  $\sigma_{11}^c$  is derived as follows (9) :

$$\sigma_{11}^c = \lambda^2 [C_{11} E_{11} + C_{12} E_{22} + C_{13} E_{33}] \quad (9)$$

The same method for the  $\sigma_{22}$  and  $\sigma_{33}$  loading cases, macroscopic strain loadings  $E$  are defined respectively by the equations (Eq. 10) to (Eq. 12).

$$\begin{aligned} E_{11} &= S_{12} \sigma_{22} \\ E_{22} &= S_{22} \sigma_{22} \\ E_{33} &= S_{23} \sigma_{22} \end{aligned} \quad (10)$$

$$\begin{aligned} E_{11} &= S_{13} \sigma_{33} \\ E_{22} &= S_{23} \sigma_{33} \\ E_{33} &= S_{33} \sigma_{33} \end{aligned} \quad (11)$$

buckling strains are given by the equations (6) and (10) for ultimate stress  $\sigma_{22}^c$  and by the equations (6) and (11) for ultimate stress  $\sigma_{33}^c$ . Ultimate stresses are derived from the equations (12).

$$\begin{aligned} \sigma_{22}^c &= \lambda^2 [C_{12} E_{11} + C_{22} E_{22} + C_{23} E_{33}] \\ \sigma_{33}^c &= \lambda^2 [C_{13} E_{11} + C_{23} E_{22} + C_{33} E_{33}] \end{aligned} \quad (12)$$

For shear loading cases, the failure stress components are defined by the equations (13) under uncoupled shear strain loadings.

$$\begin{aligned} \sigma_{13}^c &= \lambda^2 [C_{44} E_{13}] \\ \sigma_{23}^c &= \lambda^2 [C_{55} E_{23}] \\ \sigma_{12}^c &= \lambda^2 [C_{66} E_{12}] \end{aligned} \quad (13)$$

The above described method is quite general and allows to assume pure stress loading with the strain approach retained for homogenization. Nomex<sup>®</sup> predictions are successfully compared to mechanical data given by the Euro-Composites company Tab. 2 and Tab. 3).

**Table 2 :** Comparison between finite element mechanical properties (FE) and manufacturer ones (EC). Minimum (Min) and typical (Typ) out of plan shear moduli of honeycombs cores ECA-R 4.8 with densities of 29 and 64Kg/m<sup>3</sup>

ECA -R	4.8-29 (51)				4.8-64 (51)			
	Min		Typ		Min		Typ	
	FE	EC	FE	EC	FE	EC	FE	EC
$G_{13W}$	14.6	14	23.9	24	42.7	48	50.1	56
$G_{23L}$	8.6	9	14.1	14	25.1	22	29.5	26

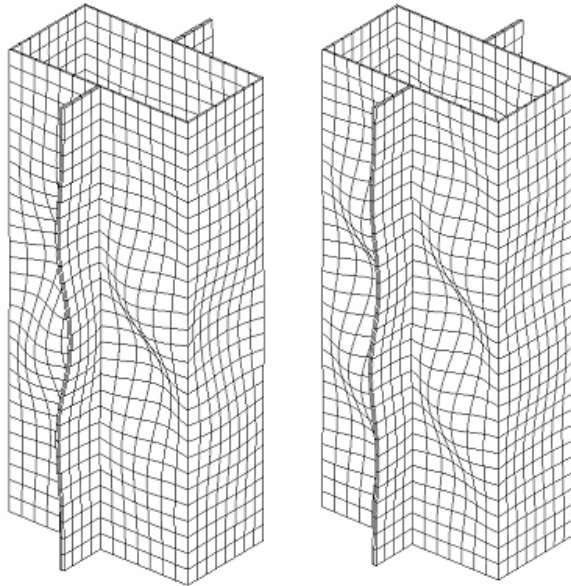


**Figure 10 :** Buckling mode of the over-expanded honeycomb RVE under shear loading  $E_{23}$ . Buckling mode of the rectangular over-expanded honeycomb RVE under shear loading  $E_{13}$ .

The second evolution of the NidaCore prototype software integrates in the RVE the interaction between the mechanical characteristics of core and face-sheets. The carbon-fibre epoxy-matrix laminated face-sheets can be constraint to simulate mechanical testing boundary conditions. The out of plan shear moduli of Over-expanded and Hexagonal RVE with T700S/M10 balanced carbon fabrics face-sheets laid with 0° or 45° compared to the orthotropic directions of the core are presented in Tab. 4.

**Table 3:** Comparison between finite element mechanical stress properties (FE) and experimental results

ECA-R	Min	Min	Typ	Typ
MPa	FE	Tests	FE	Tests
	4.8-29 (51)	4.8-29 (51)	4.8-29 (51)	4.8-29 (51)
$\sigma_{11}^C$	0.185	-	0.31	-
$\sigma_{22}^C$	0.282	-	0.48	-
$\sigma_{33}^C$	0.39	0.6	0.62	0.85
$\sigma_{12}^C$	0.72	-	1.2	-
$\sigma_{13}^C$	0.33	0.32	0.55	0.44
$\sigma_{23}^C$	0.25	0.31	0.415	0.42

**Table 4 :** ECA-R-29 (51) Mechanical properties with and without skin for 12,7 thickness

T700S/M10	$G_{23}$	$G_{13}$	$\sigma_{13}^C$	$\sigma_{23}^C$
0,36mm thickness	(MPa)	(MPa)	(MPa)	(MPa)
Rigid	14,6	8,6	0,33	0,25
face-sheets				
Laminates 0°	15,4	10,2	0,511	0,690
Laminates 45°	15,85	10,16	0,512	0,906

### 2.3 Compressive tests on sandwich specimens

In this part, a campaign of compressive tests performed on sandwiches structures made of Nomex<sup>®</sup> hexagonal honeycomb core and carbon-fibre / epoxy-resin laminated composite skins is presented. The experimental data obtained are compared with finite element results computed with the software NidaCore. The block size of Nomex<sup>®</sup> honeycomb core is 50 mm (W direction) x 40 mm (L direction) x 25 mm (T direction). It comes from Hexcel and has the following characteristics: cell size: 3.175 mm; density: 80 kg.m<sup>-3</sup> and wall thickness: 0.22 mm. Two TR-50 composite skins of thickness 0.68 mm and stacked at [ 45 -45 ] are stucked on each side of the core to complete the specimen. As a result, the specimens presented here are [ 45 -45 CORE -45 45 ] shaped. They ensure similar boundary conditions between the skins and the core as the one met in structural constructions.

The tests are carried out on a MTS hydraulic tensile testing machine ("810 material test system"). The specimens are placed between two plates of compression and crushed up to



a maximum strain of  $0.05 \text{ m.m}^{-1}$  with an imposed velocity of  $0.025 \text{ mm.s}^{-1}$ . This corresponds to a compressive quasi-static strain rate of  $1.10^{-3} \text{ s}^{-1}$ . Three stress versus strain curves are plotted on Fig. 12 below.

They show the existence of three major crushing steps. The first one, a linear growth of the stress versus strain, corresponds to the reversible elastic response of the Nomex<sup>®</sup> honeycomb core. Once a critical load is reached, corresponding to a compressive stress of roughly 3.6 MPa, a brutal decrease in stress is observed. This phenomenon is in link with the apparition of a global instability within the honeycomb core. The buckling of the walls of the whole specimen explains the abrupt loss of stiffness. After this first global collapse of the structure, a slightly rising plateau is observed.

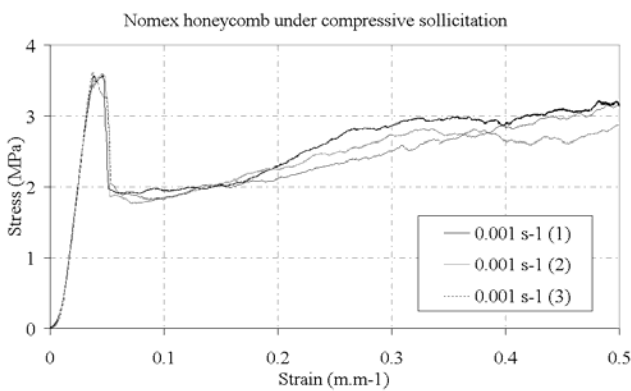


**Figure 12:** Crushed specimen and stress versus strain curve for quasi static loading

It is due to both the local buckling of the walls of the honeycombs (see Fig. 13 through the formation of buckling plies) and the densification of the core between the two skins. It can be noticed here that, if the tests are performed up to more than fifty percent of strain, the response of the specimen becomes very stiff while the densification of the crushed honeycombs grows. The last observation coming from the stress versus strain curves is that the tests give very similar results which proves the data to be reliable.

After some post-processing, the Young's modulus is estimated to 140 MPa and the crushing stress to 3.55 MPa. In Hexcel's catalogue, there is no data for thicknesses different from 12.7 mm. This demonstrates all the interest to have a reliable predictive method. However, to give an order of comparison, the Young's modulus and the crushing stress for a Nomex<sup>®</sup> honeycomb core of thickness 12.7 mm are equal to 255 MPa and 4.5 MPa respectively. Hence, the values obtained from the crushing tests seem to be coherent with the fact that when the thickness of the core goes up, the mechanical properties decrease (Young's modulus and crushing strength).



**Figure 13:** Sandwich specimen after crushing, Local buckling plies

The last step of this part deals with the finite element analysis of the specimen. The objective is to determine, thanks to the knowledge of the elastic properties of Nomex<sup>®</sup> paper, the compressive modulus of the honeycomb core and its associated crushing stress. The unit cell (the RVE) is meshed and periodic conditions are imposed on its bounds as described in 2.2. The skins are modeled as rigid solids.

Nine elementary loading cases are simulated in order to determine the elastic properties of the Nomex<sup>®</sup> honeycomb core. They are: uniaxial tensile tests ( $E_{11}$ ,  $E_{22}$  and  $E_{33}$ ), shearing tests ( $G_{12}$ ,  $G_{13}$  and  $G_{23}$ ) and biaxial tensile tests ( $E_{11}$  &  $E_{22}$ ,  $E_{11}$  &  $E_{33}$  and  $E_{22}$  &  $E_{33}$ ). The orthotropic elastic properties of the honeycomb are then deduced from these analysis thanks to the strain energy based homogenization procedure.

The crushing stress is computed thanks to a buckling analysis of the RVE. An imposed vertical displacement provides the critical compressive strain from which is deduced the crushing stress. The Tab. 7 below presents the comparison between computed values and experimental data. The results present satisfying agreement. Actually, the NidaCore software appears to be able to predict the mechanical properties of Nomex<sup>®</sup> honeycomb cores with enough accuracy.

**Table 7:** Comparison between computed values and experimental data

	$E_{33}$ (MPa)	$\sigma_{33}^C$ (MPa)
Experimental	140	3.55
Computed	180	4,1

### 3 Sailing race boats

Sailing race boats are using high technology sandwich fabrication methods based on carbon-fibre prepreg face-sheets and Nomex<sup>®</sup> or foam cores. Around the world races allow architects to innovate and optimize the sandwich structures within a minimum weight. Figure 14 shows the

finite element mesh of B1 developed at the laboratory for design checking. This multihull is the fastest ocean sailing vessel ever created. The B1 structure is well known as Orange II. In 2005, its skipper Bruno Peyron and his crew sailed around the world in 50 days 16h 20m with a sustained maximum boats speed of 42.7 knots (Jules Verne Trophy). B1 is a 120 ft monster of some 30 tonnes sandwich structure. It was launched from the Vannes based builders and designer group Multiplast six weeks before the Jules Verne Trophy. Durability consideration is a prior concern in the design part of these racing vessels. All reliable numerical tools and mechanical tests are used in order to improve the structure design. Several damage mechanisms may contribute to sandwich structure failures. Matrix cracking often appears at first in laminates. These micro-cracks may coalesce and initiate delaminations and large scale crack propagation. Interfaces between core and laminates may debond or core crushing may lead to sandwich buckling and failure. All damage mechanisms described above must be avoided under sailing condition loadings.



**Figure 14:** Finite Element Mesh of the B1 sailing race boat (Gilles Ollier Design Team, Multiplast, France)

#### 4 Conclusions

Numerical NidaCore results show that the software based on periodic homogenization techniques and RVE instability phenomena is a powerful tool very useful to determine the components of the effective elasticity tensor and the failure properties of Nomex<sup>®</sup> cores. Thank to this program, it is possible to predict all the ultimate stresses and then to draw the failure envelope of Nomex<sup>®</sup> honeycomb cores. This work represents the first step towards a global identification of a damage core model dedicated to sandwich structure predictions. An initial set of Nomex<sup>®</sup> properties was determined using NidaCore numerical predictions. It has been shown that experimental data and NidaCore finite element predicted values exhibited strong correlation for

classical Nomex<sup>®</sup> mechanics tests conducted by honeycomb cores manufacturers.

#### 5 References:

- Kelsey S.; Gellatley RA; Clark BW** (1958): The shear modulus of foil honeycomb cores, *Aircraft Engineering*, vol. 30, 294-302.
- Gibson L.J.; Ashby MF** (1988): *Cellular solids structures and properties*, Pergamon Press. Oxford.
- Hohe J.; Becker W.** (1999): Effective elastic properties of triangular grid structures, *Composite Structures*, vol. 45, 131-145.
- Hohe J.; Becker W.** (2001): A refined analysis of the effective elasticity tensor for general cellular sandwich core, *International Journal of Solids and Structures*, vol. 38, 3689-3717.
- Grediac M.** (1993):, A finite element study of the transverse shear in honeycomb cores, *International Journal of Solids Structures*, vol. 30, 1777-1788.
- Gornet L.; Marckmann G.; Lombard M.** (2006) : Détermination des coefficients d'élasticité et de rupture d'âmes nids d'abeilles Nomex<sup>®</sup>: homogénéisation périodique et simulation numérique, *Mécanique Industrie*, vol. 6, 595-604.
- Suquet P.** (1982) : Plasticité et homogénéisation, *Doctorat d'état, Université Paris 6*.
- Nomex<sup>®</sup> cores**, <http://www.euro-composites.com>
- Hexcel** (1999) "HexWeb<sup>TB</sup> Honeycomb Attributes and properties, *Hexcel Composites*.